DOI: 10.1002/ejic.201100618

HP-KB_3O_5 Highlights the Structural Diversity of Borates: Corner-Sharing BO_3/BO_4 Groups in Combination with Edge-Sharing BO_4 Tetrahedra

Stephanie C. Neumair,[a] Stefan Vanicek,[a] Reinhard Kaindl,[b] Daniel M. Többens,[c] Charlotte Martineau,[d] Francis Taulelle,[d] Jürgen Senker,[e] and Hubert Huppertz*[a]

Keywords: Borates / High-pressure chemistry / X-ray diffraction

The new compound HP-KB_3O_5 was synthesized under high-pressure/high-temperature conditions. It is the first compound exhibiting all three possible conjunctions simultaneously: corner-sharing BO_3 groups, corner-sharing BO_4 units, as well as edge-sharing BO_4 tetrahedra. Calculations of harmonic vibrational frequencies and ^{11}B solid-state NMR measurements were performed for the first time with a compound exhibiting edge-sharing BO_4 tetrahedra.

Introduction

The vast majority of syntheses in solid-state chemistry are performed by the variation of the thermodynamic parameters, composition, and temperature. The technically much-more demanding manipulation of the parameter pressure opens up tremendous possibilities for the synthesis of new materials. In the last decade, our high-pressure research focused on the substance class of borates, which led to a variety of new polymorphs and compounds with new compositions, not attainable under ambient-pressure conditions.[1] In contrast to ambient-pressure borates, in which trigonal BO_3 groups occur next to BO_4 tetrahedra, the new high-pressure borates predominantly exhibit boron fourfold coordinated by oxygen anions as a result of the pressure coordination rule.[2,3] Most striking was the discovery of edge-sharing BO_4 tetrahedra (B_2O_6 units) in $Dy_4B_6O_{15}$.[4] Meanwhile, this motif was observed in three different structure types represented by the high-pressure compounds $RE_4B_6O_{15}$ (*RE* = Dy, Ho),[4,5] α-$RE_2B_4O_9$ (*RE* = Sm–Ho),[6–8] and β/HP-MB_2O_4 (*M* = Fe, Ni, Co).[9–11] With the compounds $M_6B_{22}O_{39}{\cdot}H_2O$ (*M* = Fe, Co), intermediate states between corner- and edge-sharing BO_4 tetrahedra could also be isolated.[12] To our astonishment, the structural feature of edge-sharing BO_4 tetrahedra was recently found in the compound $KZnB_3O_6$, synthesized under ambient pressure conditions.[13,14] Thus, the structural motif of edge-sharing BO_4 tetrahedra is no longer a domain of high-pressure chemistry, but is still favored under these conditions, as there are eleven different compounds with three structure types prepared under high-pressure conditions and only one compound synthesized under ambient-pressure conditions. However, the synthesis of $KZnB_3O_6$[13,14] leads to the question, in principle, whether it is possible to synthesize a borate exhibiting all the above-mentioned structural motifs (corner-sharing BO_3/BO_4 groups and edge-sharing BO_4 tetrahedra) simultaneously. With HP-KB_3O_5 (HP = high pressure), we synthesized a new borate, in which the two well-known fundamental structural motifs, alias BO_3 and BO_4 groups, and all noted conjunctions, namely corner-sharing of BO_3/BO_4 groups and corner- as well as edge-sharing of BO_4 tetrahedra, are discovered in one crystal structure for the first time. This occurred in the scope of pressure-induced crystallization experiments on glass forming alkali borates, whilst investigating the ternary system K–B–O, where six different crystal structures are known: $K_5B_{19}O_{31}$,[15] KB_5O_8,[16,17] α-KB_5O_8,[18] $K_2B_4O_7$,[19] $K_3B_3O_6$,[20,21] and KB_3O_5.[22,23] The latter (ambient-pressure modification) is built up from rigid triborate rings consisting of two corner-sharing BO_3 triangles and a corner-sharing BO_4 tetrahedron.

[a] Institut für Allgemeine, Anorganische und Theoretische Chemie,
Leopold-Franzens-Universität Innsbruck
Innrain 52a, 6020 Innsbruck, Austria
Fax: +43-512-507-2934
E-mail: hubert.huppertz@uibk.ac.at
http://www-c724.uibk.ac.at/aac/
[b] JOANNEUM RESEARCH Forschungsgesellschaft mbH, MATERIALS – Institut für Oberflächentechnologien und Photonik,
Funktionale Oberflächen,
Leobner Strasse 94, 8712 Niklasdorf, Austria
[c] Institut für Mineralogie und Petrographie,
Leopold-Franzens-Universität Innsbruck
Innrain 52, 6020 Innsbruck, Austria
[d] Tectospin - Institut Lavoisier de Versailles (ILV), UMR CNRS 8180,
Université de Versailles St Quentin
45 Avenue des Etats-Unis, 78035 Versailles cedex, France
[e] Anorganische Chemie III, Universität Bayreuth
Universitätsstr. 30, 95447 Bayreuth, Germany
Supporting information for this article is available on the WWW under http://dx.doi.org/10.1002/ejic.201100618.

Results and Discussion

We succeeded in synthesizing the high-pressure modification HP-KB_3O_5 by a high-pressure/high-temperature reaction at 3 GPa and 600 °C in a modified Walker module. The compound was obtained as a colorless crystalline solid. The crystal structure of HP-KB_3O_5 was solved and refined by single-crystal X-ray crystallography. The crystal structure (Figure 1; view along [110]) consists of ribbons of BO_4 tetrahedra, which run along the *c* axis.

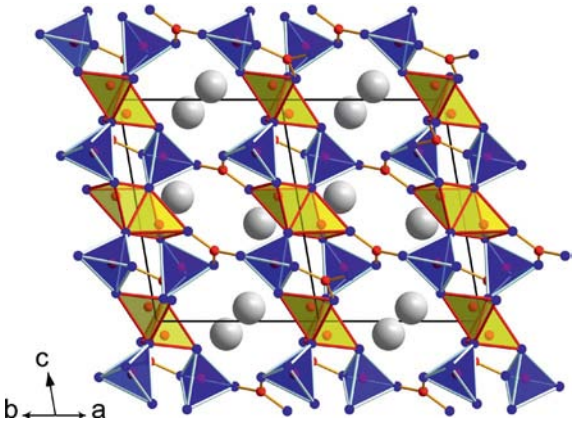

Figure 1. Crystal structure of HP-KB_3O_5 with edge-sharing BO_4 units; view along [110]. Large light spheres: K^+, corners of polyhedra: O^{2-}, small grey spheres: B^{3+}.

Within the ribbons, the BO_4 tetrahedra are connected through common corners and edges. The ribbons are interconnected by trigonal-planar BO_3 groups to form channels, in which the tenfold coordinated potassium ions are situated. The recently published $KZnB_3O_6$[13,14] shows remarkable similarities to our compound and is built up from $[B_6O_{12}]^{6-}$ groups (two rings of two BO_3 and one BO_4 unit, linked by edge-sharing BO_4 tetrahedra), which are connected by ZnO_4 tetrahedra to form a three-dimensional network. Figure 2 depicts a comparison of the crystal structures of HP-KB_3O_5 and $KZnB_3O_6$.[13,14] In HP-KB_3O_5 (Figure 2, left), the edge-sharing BO_4 tetrahedra (light polyhedra) connect to two BO_3 and four BO_4 groups through common corners. Two of the BO_4 groups are situated at the common edge of the B_2O_6 unit. It is for the first time that oxygen ions, involved in the edge-sharing of BO_4 tetrahedra, are observed to bridge three BO_4 tetrahedra ($O^{[3]}$). In $KZnB_3O_6$[13,14] (Figure 2, right), there are also edge-sharing BO_4 tetrahedra and BO_3 groups, but no corner-sharing BO_4 groups. Here, the edge-sharing BO_4 tetrahedra (light polyhedra) connect to four BO_3 units; two ZnO_4 groups are situated at the common edge of the B_2O_6 unit (highlighted with arrows).

The mean B–O distance in the BO_4 tetrahedra and the BO_3 groups of HP-KB_3O_5 is 147.7 and 137.3 pm, respectively, which agrees with the average B–O distance of the BO_4 and BO_3 units in borates (BO_4: 147.6 pm, BO_3: 137.0 pm).[24–26] Figure 3 (left) shows that the B–O distances inside the B_2O_2 rings of the B_2O_6 unit are larger [154.8(1) and 151.4(1) pm] than those outside the rings [141.2(1) and 144.6(1) pm]. The B···B distance inside the B_2O_6 unit of HP-KB_3O_5 is 221.5(1) pm, which is significantly larger than the values found in other high-pressure borates that exhibit edge-sharing BO_4 tetrahedra, e.g. $Dy_4B_6O_{15}$ [207.2(8) pm],[4] α-$Sm_2B_4O_9$ [207.1(9) pm],[8] β-FeB_2O_4 [208.3(5) pm],[9] and $KZnB_3O_6$ [207.9(4) pm].[13,14] The reason for this increased value lies in the different coordination spheres of the O ions at the common edge of the B_2O_6 unit (O1). As depicted in Figure 3 (right), the O1 anions in β-FeB_2O_4[9] are coordinated tetrahedrally in the form of two covalently bound boron atoms and two coordinating metal ions (2+2 coordination). In HP-KB_3O_5 (Figure 3, left), the O1 anions are bound covalently to three boron atoms ($O^{[3]}$), which lead to enhanced distances inside the B_2O_6 ring and therewith to a remarkably enlarged B···B distance.

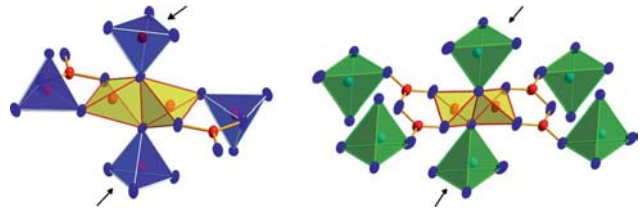

Figure 2. Comparison of the central structural motifs of HP-KB_3O_5 (left) and $KZnB_3O_6$[13,14] (right) (90% probability ellipsoids). The arrows point to the BO_4 (HP-KB_3O_5) and ZnO_4 tetrahedra ($KZnB_3O_6$), which are located at the common edge of the edge-sharing BO_4 groups.

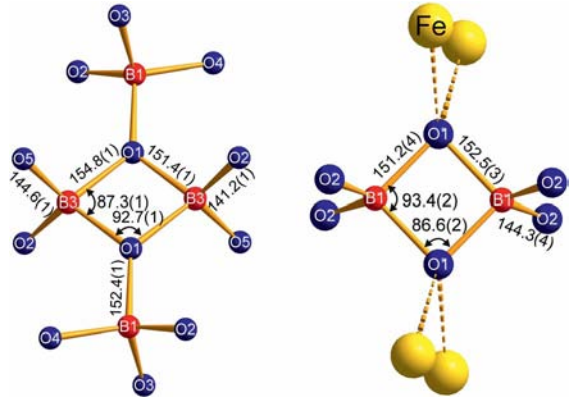

Figure 3. Comparison of selected distances [pm] and angles [°] in the B_2O_6 group of HP-KB_3O_5 (left) and β-FeB_2O_4 (right).

The potassium ions are coordinated by ten oxygen ions with distances between 264–341 pm (av. 300 pm). These values correspond to those in KV_3O_8 (272–331 pm; av. 301 pm)[27] and $K_3V_5O_{14}$ (273–335 pm; av. 300 pm).[28]

Bond-valence sums were calculated for all atoms by using the CHARDI (charge distribution in solids, $\sum Q$)[29] and bond length/bond strength concepts ($\sum V$).[30,31] The formal charges of the ions were confirmed by the calculations of both concepts.

Taking into account the synthetic conditions (3 GPa, 600 °C), we investigated the assumed metastable character of the high-pressure phase HP-KB_3O_5. Temperature-programmed X-ray powder diffraction experiments reveal that HP-KB_3O_5 is stable up to 550 °C under ambient-pressure conditions (Figure S1). Higher temperatures lead inter alia to the normal pressure phase KB_3O_5.[22] DTA measurements confirm the temperature stability of HP-KB_3O_5 (Figure S2).

Vibrational spectroscopic measurements and calculations of harmonic vibrational frequencies at the Γ point yield modes involving mainly the corner-sharing BO_3 groups above 1320 cm^{-1}, stretching vibrations of the corner- and edge-sharing BO_4 tetrahedra between 950–1215 cm^{-1}, bending and complex vibrations of both BO_3 and BO_4 units between 200–905 cm^{-1}, and lattice vibrations involving potassium below 185 cm^{-1} (Figure 4).

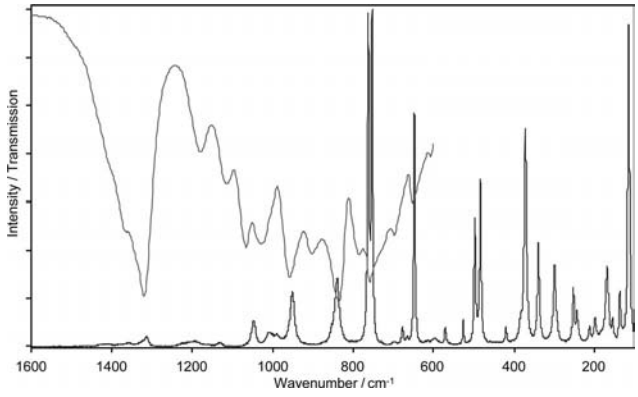

Figure 4. FTIR-ATR (top) and confocal Raman (bottom) spectra of HP-KB_3O_5. For a better comparability, the ATR-units were transformed into transmission.

The calculations enabled for the first time a precise assignment of the previously discussed vibrational modes of these B_2O_6 groups.[32,12] For example, bands at 1213, 1205, 1161, and 1013 cm^{-1} for the Raman-active modes and at 1105, 1070, and 1001 cm^{-1} for the IR-active modes can now be assigned to modes involving strong movements of the two common oxygen ions within the two edge-sharing tetrahedra. The Raman-active mode at 1213 cm^{-1} exhibits the strongest vibration within the B_2O_6 unit.

The Raman-active modes of B_2O_6 groups were investigated previously on HP-NiB_2O_4,[9] α-$Gd_2B_4O_9$,[6] and $Dy_4B_6O_{15}$.[4] The spectra of these compounds reveal several bands in the range 1200–1450 cm^{-1}, which normally correspond to BO_3 or OB_3 groups (the latter is not part of a B_2O_6 group). As none of the three compounds with edge-sharing BO_4 tetrahedra contain three-coordinate boron atoms or three-coordinate oxygen atoms, these peaks are assumed to likely be Raman-active modes of the B_2O_6 unit. A comparison of the different spectra indicates two bands that probably could be assigned to modes of edge-sharing BO_4 tetrahedra (1262 and 1444 cm^{-1} in HP-NiB_2O_4, 1253 and 1431 cm^{-1} in α-$Gd_2B_4O_9$, and 1271 and 1435 cm^{-1} in $Dy_4B_6O_{15}$). Even for the recently published $KZnB_3O_6$,[13,14] Jin et al. found an absorption band in the range 1400 cm^{-1}, but missed the weak B_2O_6 vibration at 1210 cm^{-1}. Further calculations are necessary to reveal whether the B_2O_6 units of the above-mentioned phases show bands in the region of 1400 cm^{-1}. The here discussed HP-KB_3O_5 exhibits no band around 1400 cm^{-1}, which is caused by the vibrations of the B_2O_6 unit. This difference in the spectra from those of other compounds comprising edge-sharing BO_4 tetrahedra might be due to the increased boron coordination of O1. Vibrational spectroscopy of HP-KB_3O_5 confirms the absence of water in the structure.

Until 2009, only paramagnetic compounds with edge-sharing BO_4 tetrahedra could be obtained, on which solid-state ^{11}B NMR spectroscopic investigations are impossible. Such ^{11}B solid-state NMR investigations would be of paramount interest to answer the question whether the chemical shift values and quadrupolar coupling constants of ^{11}B are sensitive enough to unequivocally identify the structural motif of the edge-sharing BO_4 tetrahedra. This would significantly simplify the investigation of technically important borate glasses. Up to now, edge-sharing BO_4 tetrahedra are unknown in borate glass chemistry.[33,34] With the two diamagnetic compounds HP-KB_3O_5 and $KZnB_3O_6$[13,14] ^{11}B solid-state NMR measurements now become possible for the first time.

Figure 5 shows a ^{11}B MQMAS spectrum for HP-KB_3O_5. The MQMAS technique allows the separation of the individual resonances of the typical broad 1D ^{11}B MAS spectra. While the F2 dimension retains the full interaction including the chemical shift and second-order quadrupole interaction, for the F1 dimension, only the isotropic chemical and quadrupolar induced shifts are relevant. For HP-KB_3O_5, both inequivalent BO_4 as well as the BO_3 units can be distinguished (Table 1). Furthermore, an evaluation of slices at δ(F1) values of 0.5, 2.5, and 22 ppm gives access to the isotropic chemical shift δ_{iso}, the quadrupole coupling constant C_Q, and the asymmetry parameter η_Q for each individual boron site (Figure 5 and Table 1). These data were then used to determine the intensity ratios by deconvoluting an 1D ^{11}B MAS spectrum recorded with selective excitation (Figure 5). In a similar procedure, the data for $KZnB_3O_6$[13,14] depicted in Table 1 were also collected. Although data analysis of $KZnB_3O_6$ was hampered by a substantial impurity of boronic acid, values for δ_{iso}, C_Q, and η_Q for the trigonal planar and tetrahedral boron units could be derived.

On the basis of investigations of minerals, some empirical values are reported for both BO_3 and BO_4 units.[35–38] While BO_3 units typically are observed between 14 and 23 ppm (δ_{iso}) and exhibit large C_Q values (2.4 to 2.9 MHz), tetrahedrally coordinated boron atoms usually range from –1 to 3.5 ppm and 0.2 to 0.5 MHz for δ_{iso} and C_Q, respectively. The asymmetry parameter η largely depends on local distortions and connectivities and can vary between 0 and 0.8 for both units. The observed values (Table 1) for HP-KB_3O_5 and $KZnB_3O_6$ fit quite well into these regions. Since for $KZnB_3O_6$[13,14] only edge-sharing BO_4 units exist, the iso-

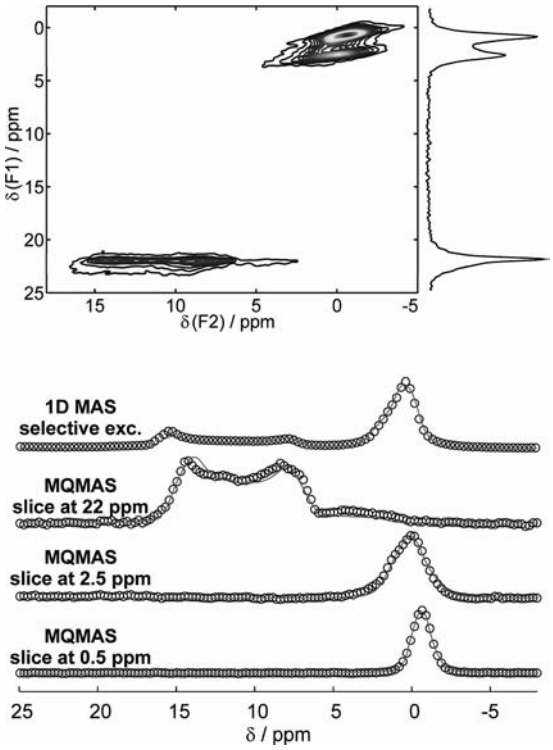

Figure 5. ^{11}B MAS NMR spectra for HP-KB_3O_5. 2D MQMAS spectrum (top) and 1D MAS spectrum with selective excitation as well as three horizontal slices of the MQMAS spectrum (bottom). The experimental data and the simulations are depicted with open circles and solid lines, respectively. The relevant refinement parameters are given in Table 1.

Table 1. Results of the refinement of the ^{11}B MQMAS and selective 1D spectra for HP-KB_3O_5 and $KZnB_3O_6$. Details of the fitting procedure are given in the text.

	Unit	δ_{iso} / ppm	C_Q / MHz	η	I
HP-KB_3O_5	BO_4	0.31(2)	0.95(5)	0.55(4)	1.08(6)
	BO_4	1.75(2)	1.2(1)	0.74(5)	0.85(6)
	$BO_3(T_2)$	16.8(2)	2.5(1)	0.17(3)	0.98(6)
$KZnB_3O_6$	BO_4	2.4(1)	0.8(1)	0.4(1)	–
	$BO_3(T_2)$	18.1(3)	2.4(1)	0.3(2)	–

tropic shift of 2.4 ppm can be assigned to those units. Probably, the resonance at δ = 1.75 ppm might accordingly be assigned to the edge-sharing BO_4 tetrahedra for HP-KB_3O_5. Nevertheless, because there are only slight variations for the second BO_4 unit, this assignment is not unequivocal. It is at least questionable whether it will be possible to detect edge-sharing tetrahedral units on the basis of ^{11}B chemical shift data. In a forthcoming study, we will combine NMR spectroscopic analysis with quantum chemical calculations of the chemical shift and the electric field gradient tensor to get a more detailed picture of the relevant interactions.

Conclusions

Systemic investigations in the field of high-pressure borates led to the synthesis of HP-KB_3O_5, the first borate exhibiting all three possible conjunctions: corner-sharing BO_3 groups, corner-sharing BO_4 units, as well as edge-sharing BO_4 tetrahedra. Vibrations of the B_2O_6 unit could be assigned in a measured spectrum through calculations of the harmonic vibrational frequencies at the Γ point. With the two diamagnetic compounds HP-KB_3O_5 and $KZnB_3O_6$, ^{11}B solid-state NMR-measurements were performed for the first time for compounds exhibiting edge-sharing BO_4 tetrahedra.

Experimental Section

Synthesis: The title compound was prepared by grinding a stoichiometric mixture of K_2CO_3 (ChemPur GmbH, Karlsruhe, Germany, 99.9%) and H_3BO_3 (Merck KGaA, Darmstadt, Germany, 99.5%) and heating it at 900 °C for 12 h to expel H_2O and CO_2. To obtain HP-KB_3O_5, the amorphous reaction product was compressed and heated in a multianvil assembly. Therefore, the sample was reground and filled into a boron nitride crucible (Henze BNP GmbH, HeBoSint® S10, Kempten, Germany). The crucible was placed into the pressure medium: a MgO octahedron (Ceramic Substrates & Components, Isle of Wight, UK) with an edge length of 18 mm. The octahedron was compressed via eight tungsten carbide cubes (TSM-10, Ceratizit, Reutte, Austria) with a truncation edge length of 11 mm (18/11 assembly). Pressure was applied by a Walker-type multianvil device and a 1000 t press (both devices from the company Voggenreiter, Mainleus, Germany). A detailed description of the assembly and its preparation can be found in ref.[39–43] For the synthesis of HP-KB_3O_5, the assembly was compressed to 3 GPa over 1.25 h and kept at this pressure for the heating period. The sample was heated to 600 °C over 10 min, kept there for 10 min, and cooled down to 400 °C over 40 min. Afterwards, the sample was naturally cooled down to room temperature by switching off the heating, followed by a decompression period of 3.75 h. The recovered pressure medium was broken apart, and the surrounding boron nitride crucible removed from the sample. The compound HP-KB_3O_5 was obtained as an air-resistant, colorless crystalline solid.

X-ray Structure Determination: Crystal structure analysis of HP-KB_3O_5: M_w = 151.53 g mol^{-1}, colorless block, 0.12 × 0.11 × 0.06 mm, monoclinic, space group: $C2/c$, a = 9.608(2), b = 8.770(2), c = 9.099(2) Å, β = 104.4(1)°, V = 742.8(3) Å^3, Z = 8, $\rho_{calcd.}$ = 2.710 g cm^{-3}, Nonius Kappa CCD, Mo-K_α radiation (λ = 0.71073 Å); graphite monochromator, $F(000)$ = 592, μ = 1.33 mm^{-1}, T = 293(2) K, multiscan, 1647 measured reflections in the range $3.2 < 2\theta < 35.0°$, 1502 unique reflections with $I < 2\sigma(I)$, R_{int} = 0.0237; the crystal structure was solved by direct methods (SHELXS-97) and anisotropically refined by a least-squares procedure against F^2 with all data, 82 refined parameters, R_1 = 0.0266 and wR_2 = 0.0635 for $F_o^2 > 2(F_o^2)$; R_1 = 0.0312 and wR_2 = 0.0650 for all F_o^2, residual electron density between –0.61 and 0.44 e Å^{-3}, GOF = 1.107. Further details on the crystal structure investigations may be obtained from the Fachinformationszentrum Karlsruhe (FIZ, 76344 Eggenstein-Leopoldshafen, Germany; Fax: +49-7247-808-666; E-mail: crysdata@fiz-karlsruhe.de), on quoting the depository number CSD-423027.

Temperature-Programmed X-ray Powder Diffraction: Temperature-programmed X-ray powder diffraction experiments were performed

on a STOE Stadi P powder diffractometer (Mo-K_α) with a computer controlled STOE furnace. The sample was enclosed in a silica-glass capillary and heated from room temperature to 500 °C in steps of 100 °C and from 500 to 1100 °C in steps of 50 °C. After reaching 1100 °C, the sample was cooled down to 500 °C in steps of 50 °C and further on to room temperature in steps of 100 °C. At each step, a powder diffraction pattern was recorded.

DTA/TG: The simultaneous differential thermal analysis and thermogravimetric (DTA/TG) measurements were performed with a Setaram TG-92 simultaneous thermal analyzer equipped with a protected DTA/TG rod (P-type thermocouple, maximum operating temperature = 1600 °C). Temperature calibration was achieved in reference to melting points of metal standards. The measurements were conducted in a helium atmosphere.

Calculations of the Vibrational Frequencies: The vibrational frequencies were computed from first principles, by using the program CRYSTAL 06,[44] Gaussian basis sets, and the B3LYP Hybrid HF-DFT functional.

IR and Raman Spectroscopy: The confocal Raman spectra of single crystals in the range 100–1500 cm^{-1} were obtained with a HORIBA JOBIN YVON LabRam-HR 800 spectrometer. The sample was excited by the 532 nm emission lines of a 30 mW Nd:YAG laser. The size and power of the laser spot on the surface were approximately 1 μm and 5 mW. The spectral resolution, determined by measuring the Rayleigh line, was 1.4 cm^{-1}. Raman bands were fitted by the built-in spectrometer software LabSpec 5 to convoluted Gauss-Lorentz functions. The accuracy of Raman line shifts was in the order of 0.5 cm^{-1}. The FTIR-ATR (Attenuated Total Reflection) spectra of single crystals in the range 600–4000 cm^{-1} were recorded with a Bruker Vertex 70 FTIR spectrometer (spectral resolution 4 cm^{-1}), attached to a Hyperion 3000 microscope. A germanium ATR-crystal with a tip diameter of 100 μm was pressed on the surface of the borate crystal with a power of 5 N, which crushed it into pieces that were μm-sized. Spectra were corrected for atmospheric influences, and an enhanced ATR correction, with the OPUS 6.5 software, was performed. Background correction and peak fitting followed via polynomial and folded Gaussian-Lorentzian functions.

^{11}B Solid-State NMR Spectroscopy: The ^{11}B solid-state NMR spectra were acquired under magic angle spinning conditions with a Bruker Avance 500 spectrometer operating at a resonance frequency of 160.461 MHz. The peak positions are given with respect to $BF_3(OEt_2)$ at 0 ppm. The 1D spectra were recorded with a 2.5 mm triple resonance MAS probe (Bruker) by applying three soft back-to-back 90 ° pulses (ν_{nut} = 10 kHz) to ensure selective excitation, while simultaneously suppressing unwanted resonances from the probe.[45] Spinning speed and recycle delay were set to 25 kHz and 40 s, respectively. To collect the MQMAS spectra, we worked with a 3.2 triple resonance MAS probe (Bruker) and a spinning speed of 20 kHz. A three-pulse sequence with two leading hard pulses (ν_{nut} = 180 kHz) and a selective 90 ° pulse (ν_{nut} = 10 kHz) was used.[46] The pulse lengths were optimized to 3.4, 1.3, and 25 μs. The 30-fold phase cycle ensured that only the desired coherence pathway $0 \rightarrow \pm 3 \rightarrow 0 \rightarrow -1$ was selected. To obtain pure absorptive spectra, we invoked the States scheme. In total, 178 fids with 60 repetitions were recorded by using a recycle delay of 6 s. The simulations of the 1D spectra and the slices of the MQMAS spectra were carried out with the program package SIMPSON.[47]

Supporting Information (see footnote on the first page of this article): Temperature-programmed powder pattern as well as DTA curve of HP-KB_3O_5.

Acknowledgments

We would like to thank Dr. G. Heymann (LFU Innsbruck) for collecting the single-crystal data, S. Sedlmaier (LMU München) for the powder diffraction measurements, and Dr. A. Sattler (LMU München) for the DTA measurements.

[1] H. Huppertz, *Chem. Commun.* **2011**, *47*, 131–140.
[2] A. Neuhaus, *Chimia* **1964**, *18*, 93–103.
[3] C. T. Prewitt, R. T. Downs, *Rev. Mineral.* **1998**, *37*, 283–317.
[4] H. Huppertz, B. von der Eltz, *J. Am. Chem. Soc.* **2002**, *124*, 9376–9377.
[5] H. Huppertz, *Z. Naturforsch. B* **2003**, *58*, 278.
[6] H. Emme, H. Huppertz, *Chem. Eur. J.* **2003**, *9*, 3623–3633.
[7] H. Emme, H. Huppertz, *Z. Anorg. Allg. Chem.* **2002**, *628*, 2165.
[8] H. Emme, H. Huppertz, *Acta Crystallogr., Sect. C* **2005**, *61*, i29.
[9] S. C. Neumair, R. Glaum, H. Huppertz, *Z. Naturforsch. B* **2009**, *64*, 883–890.
[10] J. S. Knyrim, F. Roeßner, S. Jakob, D. Johrendt, I. Kinski, R. Glaum, H. Huppertz, *Angew. Chem.* **2007**, *119*, 9256–9259; *Angew. Chem. Int. Ed.* **2007**, *46*, 9097–9100.
[11] S. C. Neumair, R. Kaindl, H. Huppertz, *Z. Naturforsch. B* **2010**, *65*, 1311–1317.
[12] S. C. Neumair, J. S. Knyrim, O. Oeckler, R. Glaum, R. Kaindl, R. Stalder, H. Huppertz, *Chem. Eur. J.* **2010**, *16*, 13659–13670.
[13] S. Jin, G. Cai, W. Wang, M. He, S. Wang, X. Chen, *Angew. Chem. 2010*, *122*, 5087–5090; *Angew. Chem. Int. Ed.* **2010**, *49*, 4967–4970.
[14] Y. Wu, J.-Y. Yao, J.-X. Zhang, P.-Z. Fu, Y.-C. Wu, *Acta Crystallogr., Sect. E* **2010**, *66*, i45.
[15] J. Krogh-Moe, *Acta Crystallogr., Sect. B* **1974**, *30*, 1827–1832.
[16] J. Krogh-Moe, *Acta Crystallogr.* **1965**, *18*, 1088–1089.
[17] J. Krogh-Moe, *Ark. Kemi.* **1959**, *14*, 439–449.
[18] J. Krogh-Moe, *Acta Crystallogr., Sect. B* **1972**, *28*, 168–172.
[19] J. Krogh-Moe, *Acta Crystallogr., Sect. B* **1972**, *28*, 3089–3093.
[20] W. H. Zachariasen, *J. Chem. Phys.* **1937**, *5*, 919–922.
[21] W. Schneider, G. B. Carpenter, *Acta Crystallogr., Sect. B* **1970**, *26*, 1189–1191.
[22] R. S. Bubnova, V. S. Fundamenskii, S. K. Filatov, I. G. Polyakova, *Dokl. Akad. Nauk* **2004**, *398*, 643–647.
[23] J. Krough-Moe, *Acta Crystallogr.* **1961**, *14*, 68.
[24] E. Zobetz, *Z. Kristallogr.* **1990**, *191*, 45–57.
[25] F. C. Hawthorne, P. C. Burns, J. D. Grice in "The Crystal Chemistry of Boron", *Boron: Mineralogy, Petrology and Geochemistry, Vol. 33*, 2nd ed. (Eds.: E. S. Grew, L. M. Anovitz), Mineralogical Society of America, Washington, **1996**, pp. 41.
[26] E. Zobetz, *Z. Kristallogr.* **1982**, *160*, 81–92.
[27] Y. Oka, T. Yao, N. Yamamoto, *Mater. Res. Bull.* **1997**, *32*, 1201–1209.
[28] A. M. Byström, H. T. Evans Jr., *Acta Chem. Scand.* **1959**, *13*, 377–378.
[29] R. Hoppe, S. Voigt, H. Glaum, J. Kissel, H. P. Müller, K. J. Bernet, *J. Less-Common Met.* **1989**, *156*, 105–122.
[30] I. D. Brown, D. Altermatt, *Acta Crystallogr., Sect. B* **1985**, *41*, 244–247.
[31] N. E. Brese, M. O′Keeffe, *Acta Crystallogr., Sect. B* **1991**, *47*, 192–197.
[32] H. Huppertz, G. Heymann, *Solid State Sci.* **2003**, *5*, 281–289.
[33] A. C. Wright, *Phys. Chem. Glasses* **2010**, *51*, 1–39.
[34] A. C. Wright, G. Dalba, F. Rocca, N. M. Vedishcheva, *Phys. Chem. Glasses* **2010**, *51*, 233–265.
[35] S. Kroeker, J. F. Stebbins, *Inorg. Chem.* **2001**, *40*, 6239–6246.
[36] D. Müller, A. R. Grimmer, U. Timper, G. Heller, M. Shakibaie-Moghadam, *Z. Anorg. Allg. Chem.* **1993**, *619*, 1262–1268.
[37] M. R. Hansen, T. Vosegaard, H. J. Jakobsen, J. Skibs, *J. Phys. Chem. A* **2004**, *108*, 586–594.
[38] M. R. Hansen, G. K. H. Madsen, H. J. Jakobsen, J. Skibs, *J. Phys. Chem. A* **2005**, *109*, 1989–1997.

[39] N. Kawai, S. Endo, *Rev. Sci. Instrum.* **1970**, *41*, 1178–1181.
[40] D. Walker, M. A. Carpenter, C. M. Hitch, *Am. Mineral.* **1990**, *75*, 1020–1028.
[41] D. Walker, *Am. Mineral.* **1991**, *76*, 1092–1100.
[42] D. C. Rubie, *Phase Transitions* **1999**, *68*, 431–451.
[43] H. Huppertz, *Z. Kristallogr.* **2004**, *219*, 330–338.
[44] R. Dovesi, V. R. Saunders, C. Roetti, R. Orlando, C. M. Zicovich-Wilson, F. Pascale, B. Civalleri, K. Doll, N. M. Harrison, I. J. Bush, Ph. D′Arco, M. Llunell, *CRYSTAL06 - User's Manual*, University of Torino, Torino, **2006**.
[45] S. Zhang, X. L. Wu, M. Mehring, *Chem. Phys. Lett.* **1990**, *173*, 481–484.
[46] J. P. Amoureux, C. Fernandez, S. Steuernagel, *J. Magn. Reson., Ser. A* **1996**, *123*, 116–118.
[47] M. Bak, J. T. Rasmussen, N. C. Nielsen, *J. Magn. Reson.* **2000**, *147*, 296–330.

Received: June 20, 2011
Published Online: August 5, 2011

